Mohammad ARESTEH[1], Abdolreza RAHMATI[1], Shahrokh FARHANGI[2], Adib ABRISHAMIFAR[1]

Iran University of Science and Technology (1), Tehran University (2)

Bearing current reduction in a five level flying capacitor DTC drive

Abstract. *Bearing currents in induction motors caused by breakdown of thin layers of grease (electrical discharge machining) known as the main factor in bearing damage and is a function of common mode voltage (CMV). In this paper various switching tables to reduce CMV and thus bearing currents in a DTC-controlled five-level drive are compared and a new switching table using redundancy concept is presented which efficiently reduces the CMV. The simulation results in SIMULINK/Matlab environment prove the capability of the proposed strategy for reducing the common mode voltage in a five level inverter. The experimental results of a prototype five level flying capacitor inverter confirm common mode reduction using the proposed switching table.*

Streszczenie. *Prądy łożyskowania w silniku indukcyjnym powodowane przebiciem w cienkiej warstwie smaru są jedną z głównych przyczyn uszkodzenia łożysk i jest funkcją składowej wspólnej napięcia CMV. W artykule zaprezentowano tabele przełączeń umożliwiającą redukcję CMV w sterowniku bezpośredniej kontroli momentu DTC. Wyniki symulacji i eksperymentów potwierdziły możliwość redukcji CMW w pięciopoziomowym przekształtniku. (**Redukcja prądu łożyskowania w napędzie DTC**)*

Keywords- Direct torque control, Flying-capacitor multilevel inverters, Common mode voltage, Bearing current
Słowa kluczowe: bwzpośrednia kontrola momentu DTC, prądy łożyskowania.

Introduction

In industrial countries more than 70% of electrical energy is consumed by electric motors. About 60% of this amount is related to high-power pumps and fans which often are fed by medium voltage induction motors. To regulate pressure and flow, generally mechanical instruments such as throttle valve and damper were used but these methods in addition of intense pressure on mechanical devices and accelerating their depreciation, resulting in high energy losses. Nowadays due to rising energy prices, much attention has been paid to the speed control of medium voltage motors by multilevel drives. Development of this drives began in last decade using the GTO and today IGCT and high voltage IGBT with the well switching features, simplicity of control and low losses are replaced [1]. Although numerous structures are provided for medium voltage drives, but three structures of diode-clamped, H-bridge and flying capacitor find more application and are commercially available [2]-[5]. Among the above structures, flying capacitor inverter as shown in Fig. 1 has been interested because it does not require the complex transformer as cascaded H-bridge inverter and it does not generate distortion as diode-clamped. It is more attractive in high switching frequencies where leads to use the smaller capacitors. The even distribution of losses among the switches and the high frequency of the first carrier band make this topology attractive for some applications such as high speed drives.

Among the methods of induction motor speed control, direct torque control (DTC) strategy is also used in multilevel drives [6]-[8]. DTC strategy in [8] is implemented using a five-level flying capacitor inverter, but problems such as bearing currents which cause the premature failure of electrical motors has not been addressed [9]-[10]. Bearing currents under nominal frequency sine-wave operation has been recognized since 1924[9]. These currents, arising from the magnetic asymmetry in motor, can damage the bearing. In PWM VSI drives there is a different mechanism of producing bearing currents due to inverter-generated common-mode voltages. Generation of this bearing current can be illustrated using Fig. 2. Assuming the point 'o' as a reference, the CMV at phase a is V_{ao}. In practice this point is not grounded but it forms the common mode path in high frequencies through Z_{in} (due to parasitic capacitors between point ‘o’ and the grounded frame). The elements of C_{ws} and C_{wr} are the parasitic coupling capacitances from the motor windings to the stator and rotor irons, respectively. There is also a capacitance C_g across the bearings, denoting the motor air gap capacitance. The bearings are approximated by a switch B that turns on and off randomly, based on electric behavior of motor bearings [10]0.

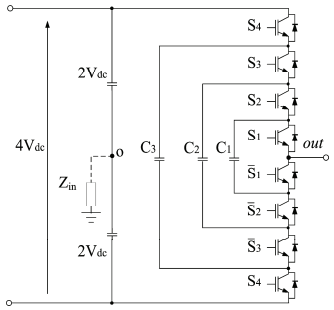

Fig.1. One leg of a 3-phases flying capacitor inverter.

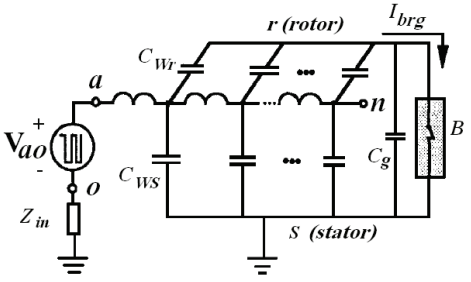

Fig.2. Principle of bearing current generation in electrical drive [10].

A closed loop circuit is formed for I_{brg} flowing into C_{wr} via bearing back to grounded stator. Similarly V_{bo} and V_{co} contribute to the bearing current [10]. Mechanism of producing bearing currents in multilevel drives as like as two-level PWM drives is due to the inverter-generated CMV. So far several methods to deal with the bearing current in low voltage drives are provided and can be classified into two groups: bearing current elimination techniques and methods of bearing current reduction. The electrostatic-shielded induction motor offers one solution and reduces the rotor shaft voltages to levels below the bearing lubricant electric field breakdown, therefore reduces the bearing wear

caused by PWM VSI drives [11]. Another method for mitigating the bearing current is neutral grounding solidly or through the impedance [12]. Common mode filter at inverter output results in sinusoidal waveform and attenuates the CMV [13]-[15]. The elimination method places the reliable shaft-riding brushes for shaft grounding to deviate the current path from the bearing directly into the stator [16]. This can be effective, but causes maintenance issues. Another method, for eliminating the bearing current, is using two insulated motor bearings [16]. Finally, the active cancellation techniques have been proposed using power electronics to reduce the CMV to zero [17].

Although, all these methods are also applicable in multilevel drives, but in multilevel drives a more cost-effective method exists due to a large number of available space voltage vectors. Therefore it is possible to get a low CMV using only some vectors and neglecting the others [18]-[20]. This paper compares a DTC strategy with various switching tables and then propose a new table which uses the concept of redundancy to get a low CMV. Thus the CMV is reduced so that it does not damage the bearing.

This paper is organized as follow. First, DTC and the effect of space vectors on the torque and flux are discussed. Then, switching table design to reduce CMV is presented. Finally simulation and practical results confirming the proposed theory are given.

Direct Torque Control in Multilevel Drives

In a three-phase symmetrical induction motor, electromagnetic torque can be expressed by:

$$T_e = \frac{3}{2} p \frac{L_m}{\sigma L_s L_r} |\overline{\psi}_s| |\overline{\psi}_r| Sin\delta_\psi \quad (1)$$

where $|\overline{\psi}_s|$ and $|\overline{\psi}_r|$, are the stator and rotor flux amplitude respectively and δ_ψ, the angle between two flux vectors, is called the torque angle. L_m, L_s and L_r are the magnetizing, stator and rotor inductances, respectively and σ is the total leakage factor of the motor defined as:

$$\sigma = 1 - \frac{L_m^2}{L_s L_r} \quad (2)$$

In DTC, flux amplitude is maintained at about nominal value and the torque is set with the torque angle. Obviously maximum torque is achieved for $\delta_\psi = \pi/2$. As we will see, the torque angle and consequently the torque is adjustable using the stator voltage vector. Stator voltage equation is given by:

$$\overline{u}_s = r_s \overline{i}_s + \frac{d\overline{\psi}_s}{dt} \quad (3)$$

Although an accurate model should use the (3), only to a simple description of DTC strategy by neglecting the first term (which is a valid approximation especially at high speeds):

$$\frac{d\overline{\psi}_s}{dt} \approx \overline{u}_s \Rightarrow \overline{\psi}_s \approx \overline{\psi}_{s0} + \overline{u}_s \Delta t \quad (4)$$

In multilevel drives like two-level drives, the stator flux trajectory can be controlled by selecting the appropriate stator voltage vectors. In this paper, the stator voltage equation is considered in the rotating reference system based on stator flux in which d-component is along the stator flux as shown in Fig. 3. Voltage vector d-component only affects the flux amplitude and its q-component changes the angle of the stator flux vector as (5):

$$\frac{d \prec \overline{\psi}_s}{dt} = \omega_{ms} = u_{sq} / |\overline{\psi}_s| \quad (5)$$

where $\angle\overline{\psi}_s$ is the position angle of the stator flux vector and u_{sq} is the q-component of vector ūs. Vector ūs has not immediate effect on the rotor flux vector. The change of rotor flux position angle related to the stator current is given by [21]:

$$\frac{d\angle\overline{\psi}_r}{dt} = \omega + \frac{L_m}{T_r |\overline{\psi}_r|} i_{sq} \quad (6)$$

where $\angle\overline{\psi}_r$ is the position angle of $\overline{\psi}_r$, ω is the rotor electrical speed, T_r is the rotor time constant, and i_{sq} is the q-component of the $\overline{i}_s$ with respect to the stator flux axis. $\bar{u}_s$ develops i_{sq} with a delay related to the leakage time constant of the stator while the mechanical time constant of the drive inhibits fast change of ω.

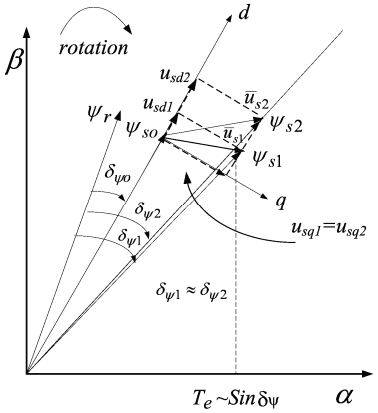

Fig. 3. Impact of stator voltage vectors on torque

At high speeds, the rotor flux position is influenced by ω, but at the low speed the rotor flux position is determined by q-component of the stator current vector (after the rotor time constant). In other words, the q-component and d-component affect the torque and flux amplitude respectively. If d- and q- components of the flux vector incremental are shown with $\Delta\psi_{sd}$ and $\Delta\psi_{sq}$ respectively, then:

$$\begin{cases} \Delta\psi_{sd} = u_{sd}\Delta t \\ \Delta\psi_{sq} = u_{sq}\Delta t \end{cases} \quad (7)$$

Torque angle variation is determined by the q-component of flux. In Fig. 3, assuming that the stator flux vector is in position of $\overline{\psi}_{s0}$, applying $\bar{u}_{s1}$ and $\bar{u}_{s2}$ vectors considering that their q- component is equal, has a same effect on the torque. Both vectors increase the flux amplitude, but d-component of $\bar{u}_{s2}$ is larger than d-component of vector ūs1 and therefore the flux changes resulting from $\bar{u}_{s2}$ will be faster. According to (4) $\bar{u}_{s2}$ changes the stator flux vector position immediately, but the rotor flux affected after delay due to the rotor time constant. Thus, assuming that the system response is faster than the rotor time constant, the rotor flux can be assumed constant during this period. If size of u_{sq} is large, consequently the amount of $\Delta\psi_{sq}$ is large and the stator flux vector keep away from the rotor flux vector and the torque will be increased. Applying u_{sq} with the average size, the value $\Delta\psi_{sq}$ is moderate, so according to the rotation of the rotor flux vector there is not a considerable change in the torque angle. If usq is small size, the amount of $\Delta\psi_{sq}$ will be low, so the torque angle δ_ψ and torque will be reduced.

Compared with two-level inverters, there is a large number of vectors with different sizes in multilevel inverters

that they can control the flux vector with different speeds and in different directions. Thus the multilevel drives have a faster and more precise control on the flux and torque. Stator voltage vector in a multilevel drive is as follow:

$$\bar{u}_s = u_a e^{j0} + u_b e^{j2\pi/3} + u_c e^{j4\pi/3} \quad (8)$$

This space vector can be indicated as number cba in which a, b and c, respectively, show the size of the voltage levels in each phase. All the space voltage vectors other than the redundant vectors for a five-level drive is shown in Fig. 4. Now, we can consider the effect of different vectors on torque and speed and determine the switching table. Assuming that the stator flux vector is entered in sector $\theta 1$ along the a-axis and direction of rotation in clockwise direction, at the first, vectors which increase the flux are investigated. In this case all the vectors in $\alpha>0$, $\beta>0$ increase the flux.

Regarding to Fig. 4, the group vectors 10x ,20x ,30x and 40x, respectively have u_{sq} component of too small, small, medium and large. According to previous explanations, with u_{sq} large to small, respectively, there is a large to a low change in stator flux position. However, the torque angle as (6) also depends on the rotor speed. For example, in the average speeds a medium-size u_{sq} can increase the torque angle and consequently the amount of torque, but at high speeds, the same usq causing the torque to be reduced. Therefore applying the proper u_{sq} will be subjected to the rotor speed.

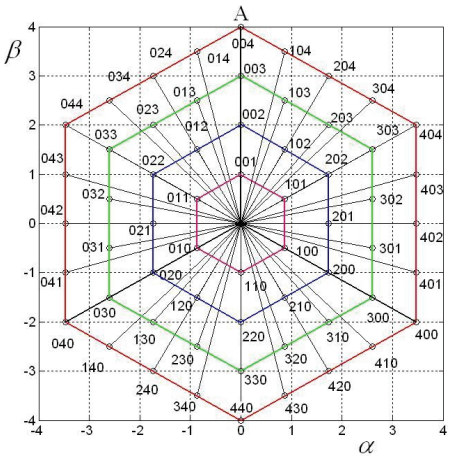

Fig.4. voltage space vectors without redundancy in a five-level inverter

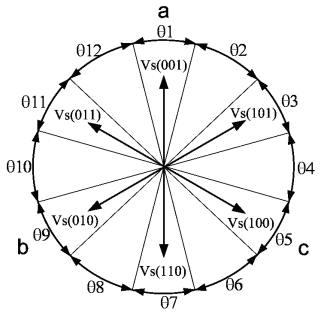

Fig.5. Multilevel DTC Sector division 0[8]

In [8], a control strategy is proposed in order to fulfill the requirements imposed by DTC when a five-level flying-capacitor inverter is used. The $\alpha\beta$ plane has been divided into 12 sectors as shown in Fig. 5. The speed of the stator flux linkage vector is given by the modulus of the applied space voltage vector. Thus, the space voltage vectors are chosen according to the rotor speed range. Voltage vectors with small amplitudes are chosen for low speeds, and vectors with bigger amplitudes are chosen for higher speeds. Taking into account the available space voltage vector amplitudes in a five-level inverter, four different tables are used so that each table corresponds to a specific speed range. However, considering that high power fans and pumps operate normally above 60% nominal speed, we focus only on high speed table [22]. For high speed range, the proper vectors are shown in Table 1, corresponding to Fig. 4 and Fig. 5. TI (torque index) and FI (flux index) show the current state of torque and flux. The value of '1' means that the torque or flux must be decreased and '-1' means that it must be increased. TI=0 means that the torque is in the acceptable range. In every sector, an appropriate voltage vector will be assigned to keep the flux and torque references as needed.

Switching table design to reduce CMV

The five-level flying capacitor inverter shown in Fig. 1, can generate a balanced three-phase positive-sequence (differential mode) voltage, also inherently produces a zero-sequence CMV. The abc phase voltages respect to the drive midpoint 'o' can be decomposed into0 [18]:

$$\begin{aligned} V_{ao} &= V_{an} + V_{no} \\ V_{bo} &= V_{bn} + V_{no} \\ V_{co} &= V_{cn} + V_{no} \end{aligned} \quad (9)$$

Where V_{no} is the equivalent common-mode voltage:

$$V_{no} = (V_{ao} + V_{bo} + V_{co})/3 \quad (10)$$

The effect of each level on the CMV can be derived as shown in Table 2 (1pu=V_{dc}/3). For example the 004 vector has level 0 in c phase, level 0 in phase b and level 4 in phase a. Therefore using (10), the CMV is equal to:

$$V_{no} = (-2V_{dc} - 2V_{dc} + 2V_{dc})/3 = -\frac{2}{3}V_{dc}$$

As can be seen from Table 1, [8] uses all rows of Table 2 other the first row. So the CMV has a peak to peak of (1pu-(-4pu))=5pu. One solution is that the vectors in rows 5, 6 and 7 were not used and instead the adjacent vectors be replaced. In this case a peak to peak of (1pu-(-1pu)) = 2pu can be obtained; the first row still not be applied. However this solution degrades the performance of the drive because adjacent vectors cannot generate required torque or have a high CMV.

Another solution to look carefully at Table 2 is obtained. if the large vectors inscribed in the outer hexagonal is used, the CMV is reduced because these vectors are not in rows 6 and 7 with a high CMV. In the previous work [8] been stated: "The speed of the stator flux linkage vector is given by the modulus of the applied space voltage vector. Thus, the space voltage vectors will be chosen according to the rotor speed. Voltage vectors with low amplitude will be chosen for low speeds, and vectors with greater amplitude will be chosen for higher speeds." However, according to (5), the speed of the stator flux linkage vector depends on the q-component of the applied stator voltage vector not on its modulus. To clarify it, assuming that the stator flux is in the point A (see Fig. 6), the vectors 202 and 204 have the same effect on the torque, although 204 increases fast the stator flux amplitude. So, the large amplitude vector 204 (which leads to low CMV) can be applied instead of the low amplitude vector of 202 in the sector θ1. Similarly, the large amplitude vector 304 can be applied instead of the medium amplitude vector 302 in the sector θ1.

Table 1. 12-Sector switching table for high speed range [8]

TI	FI	θ1	θ2	θ3	θ4	θ5	θ6	θ7	θ8	θ9	θ10	θ11	θ12
0	1	301	310	320	230	130	031	032	023	013	103	203	302
0	-1	302	301	310	320	230	130	031	032	023	013	103	203
1	1	200	210	220	120	020	021	022	012	002	102	202	201
1	-1	202	201	200	210	220	120	020	021	022	012	002	102
-1	1	401	410	430	340	140	041	043	034	014	104	304	403
-1	-1	403	401	410	430	340	140	041	043	034	014	104	304

Table 2. CMV due to different voltage vectors (1pu=V_{dc}/3)

	Applied vector	CMV
1	404,044,440	2pu
2	304,430,340,403,034,043	1pu
3	204,402,420,240,042,024,303,033,330	0
4	104,410,401,140,041,014,023,032,320,302,203,230	–1pu
5	004,400,040,103,130,301,310,013,031,202,220,022	–2pu
6	102,201,210,021,012,120,003,030,300	–3pu
7	002,200,020	–4pu

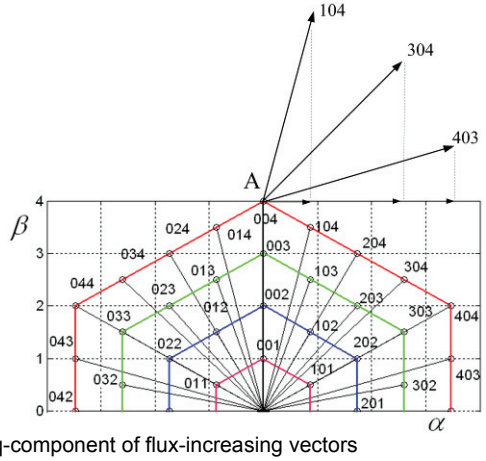

Fig. 6: q-component of flux-increasing vectors

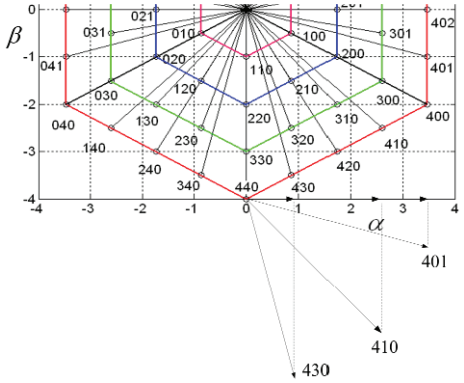

Fig. 7: q-component of flux-deccreasing vectors

Considering that the q-component of the voltage vector affects the electromagnetic torque and the d-component affects the flux amplitude, the vector 403 results in a high electromagnetic torque that accelerates the motor. On the other hand the vector 304 has a negligible effect on the electromagnetic torque. Finally, the vector 104 results in a low flux-speed so that the angles of the stator-flux and rotor-flux vectors and consequently electromagnetic torque will be decreased. All of these flux-increasing vectors have almost the same amplitude but their angles are different. In this manner, if the rotor flux is in point A (sector 1), the vectors 401, 410 and 430 decrease the flux but affect the electromagnetic torque same as 104,304 and 401, accordingly. Therefore, a new switching table, as Table 3, is proposed to perform DTC, while producing lower CMV. However, although the CMV decreases as well, but it has two major drawbacks.

Table 3. Proposed DTC switching table using large vectors

TI	FI	θ1	θ2	θ3	θ4	θ5	θ6	θ7	θ8	θ9	θ10	θ11	θ12
0	1	410	430	340	140	041	043	034	014	104	304	403	401
0	-1	304	403	401	410	430	340	140	041	043	034	014	104
1	1	430	340	140	041	043	034	014	104	304	403	401	410
1	-1	104	304	403	401	410	430	340	140	041	043	034	014
-1	1	401	410	430	340	140	041	043	034	014	104	304	403
-1	-1	403	401	410	430	340	140	041	043	034	014	104	304

Firstly, because the d-components are large, the flux varies rapidly and needs to deal with the increased switching frequency or torque ripple will increase. Secondly dv size in the inverter output be increased. For example, changing of the $TI = 0$, $FI = 1$ to $TI = 0$, $FI = -1$, a-phase output voltage is changed as big as $4V_{dc}$ which, according to the reflection theory, leading to stator overvoltages that can cause premature failure in the stator insulation.

Table 4. Proposed DTC switching table using redundancy

TI	FI	θ1	θ2	θ3	θ4	θ5	θ6	θ7	θ8	θ9	θ10	θ11	θ12
0	1	**412**	**421**	320	230	**241**	**142**	032	023	**124**	**214**	203	302
0	-1	302	**412**	**421**	320	230	**241**	**142**	032	023	**124**	**214**	203
1	1	**311**	**321**	**331**	**231**	**131**	**132**	**133**	**123**	**113**	**213**	**313**	**312**
1	-1	**313**	**312**	**311**	**321**	**331**	**231**	**131**	**132**	**133**	**123**	**113**	**213**
-1	1	401	410	430	340	140	041	043	034	014	104	304	403
-1	-1	403	401	410	430	340	140	041	043	034	014	104	304

The CMV can be reduced using redundancy concept which according that adding a same voltage to any component of a vector does not affect the differential mode voltage, but the common mode be changed. For example, vector 200 has a redundant vector 311 or 411. According to (10), by adding V_{dc} to each component, the CMV will be increased by V_{dc}. Therefore to decrease the CMV toward zero, we add a V_{dc} to each component of vectors located in rows of 5,6 and 7. So, the CMV is between -1pu and +2pu. The largest CMV is associated to vectors of 404, 044 and 440 which have not a redundant vector to reduce the CMV. The control strategy can ignore these vectors. Considering the high density of vectors in five-level drive, removal of these vectors which are located in the over-modulation area will not reduce significantly the drive capability. With the replacement of redundant vectors shown as bold font, Table 4 is obtained which in the maximum CMV is 1pu. However, the criterion in bearing corrosion is current density j_b (11) in which BVR (Bearing Voltage Ratio) is fraction of the common mode voltage that drops on the bearing and is smaller than 0.1 [23]. The oil electrical resistance after the breakdown, R_b, is in about 10 ohms. The herzian contact area, A_H, is proportional to the square of motor size ($A_H \approx h^2$):

$$j_b = \frac{BVR \bullet V_{com}}{R_b \bullet A_H} \tag{11}$$

With a 600V DC bus, 1pu= 50V. On the other hand bearing voltage ratio (BVR) is smaller than 0.1 and therefore the rotor shaft voltage is less than 5V voltage which will be less than the breakdown voltage in bearings. In medium voltage motors, although the CMV will be higher (for example 500V) but due to increasing the hertzian contact area in bearings, the bearing current density is small and rarely will cause corrosion of bearings. However, although any voltage above the breakdown voltage is leading to dielectric breakdown, but the corrosion volume per discharge is a function of voltage squared [23]. Thus the common mode voltage reduction in any amount is leading to reduced corrosion and increased bearing life.

Simulation and experimental results

The proposed strategy is verified by simulation and experiment, using a low-scale five-level flying capacitor inverter. A three-phase induction motor 3kW, 400V is accelerated to 0.85 of its nominal speed and the results of both strategies are given. The motor and DTC parameters can be found in appendix A. The block diagram of the multilevel DTC drive is shown in Fig. 8. Fig. 9 shows the stator current and rotor speed using the Table 1. The related CMV shown in Fig. 10 as a fraction of the total DC supply voltage, is asymmetric.

Fig. 11 shows the stator current and rotor speed using the switching Table 4. As can be seen, the response is almost the same as Fig. 9. The related CMV in Fig. 12, shows a considerable reduction of negative peak and is symmetric relative to zero. As compared with Fig. 10, a 60% reduction in CMV is resulted without degrading the performance of DTC drive.

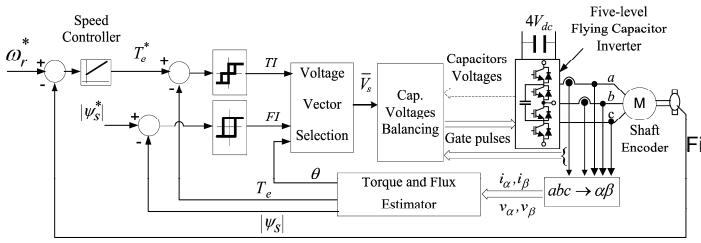

Fig. 8: Typical configuration of a multilevel DTC drive

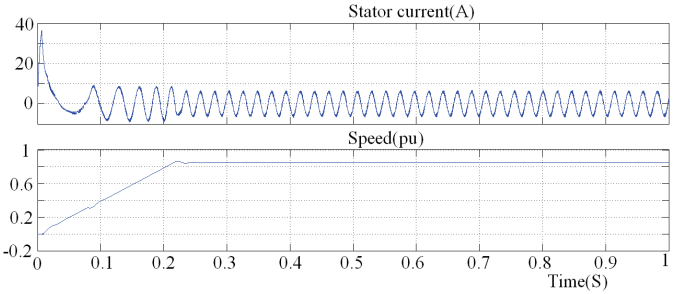

Fig. 9: Motor speed and stator current using the switching table 1

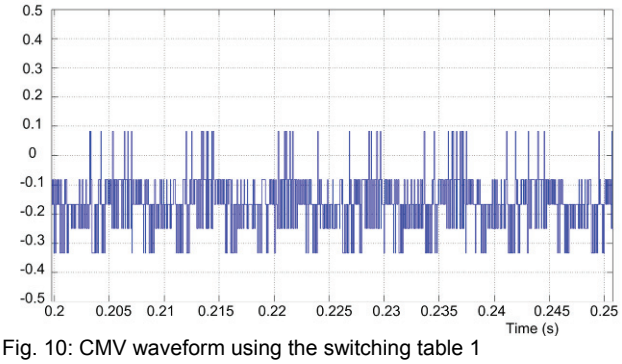

Fig. 10: CMV waveform using the switching table 1

To verify the merit of the proposed strategy, an experimental set-up was also implemented as shown in Fig. 13. The main parts of the set-up have been illustrated by the appropriate texts. The drive consist of a data-starter kit (esdspF2812), an IGBT-based flying capacitor inverter, a standard 4 HP squirrel cage induction machine, and a coupled dc machine as the mechanical load. A brief design procedure of the power circuit is given in Appendix B.

Again the motor was accelerated to 0.85pu of the nominal speed. The speed profiles using switching tables 1 and 4 are given in Fig. 14 (a) and (b), respectively. Both of them follow the speed command very well, without a noticeable overshoot or undershoot. The CMV waveforms are captured by the digital oscilloscope (50MHz, 100MS/s) and are presented for the conventional and proposed methods in Fig. 15 and 16, respectively. Reduction of the CMV amplitude using table 4 is evident in Fig. 16. The proposed method has not only decreased the amplitude of the CMV, but also its frequency. This fact is quite distinguishable from the Fig. 15 and 16. Therefore, the proposed method is quite effective in reducing the bearing current. The investigations show the capacitor balancing does not impair by the proposed strategy and is the same as before. Speed profile in proposed method shows a less measurement noise than conventional method. This is repeated in several practical test and the results were the same. It can show the reduced EMI due to CMV reduction in proposed strategy.

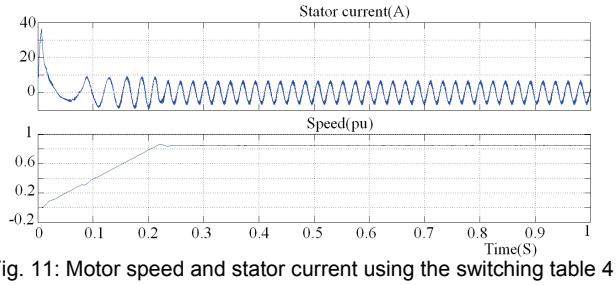

Fig. 11: Motor speed and stator current using the switching table 4

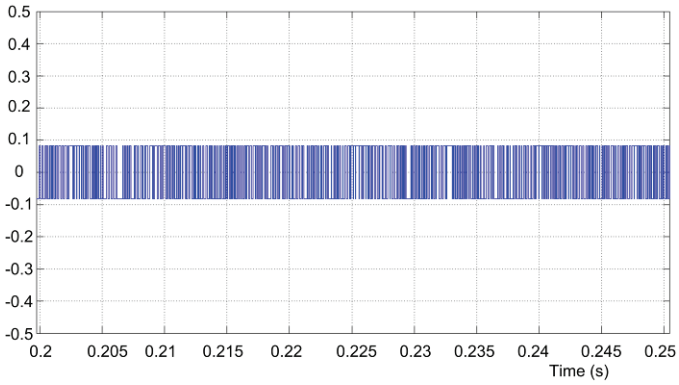

Fig. 12: CMV waveform using the switching table 4

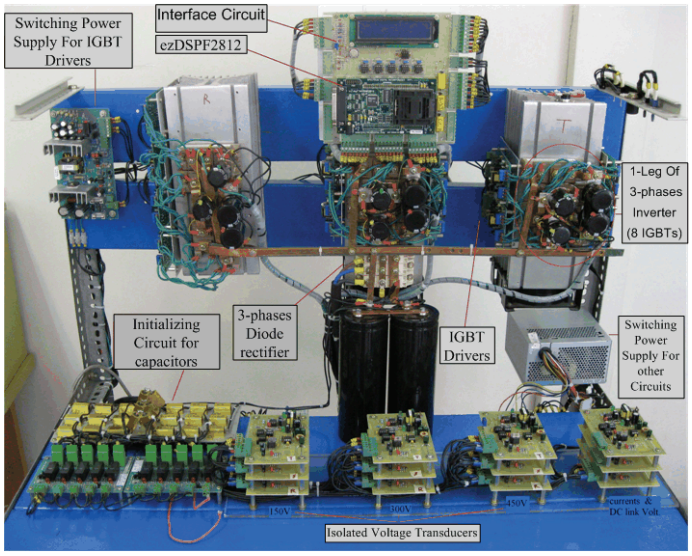

Fig. 13: Five-level flying capacitor experimental set-up

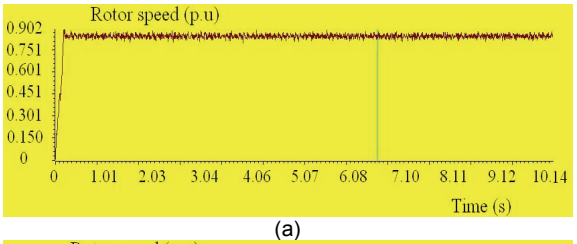

(a)

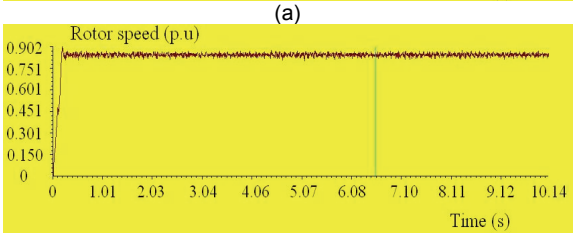

(b)

Fig. 14: Speed profiles realized by the experimental set-up: (a) conventional modulation strategy (b) proposed method

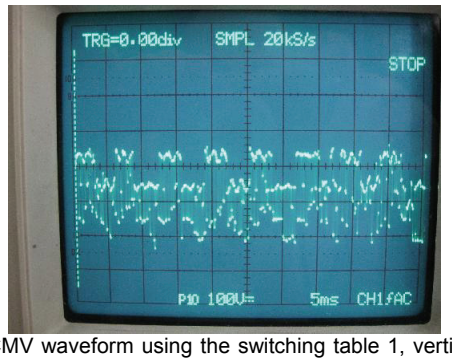

Fig. 15: CMV waveform using the switching table 1, vertical scale: 100V/div, horizontal scale: 5ms/div

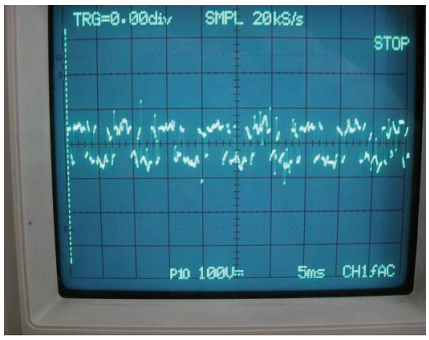

Fig. 16: CMV waveform using the switching table 4, vertical scale: 100V/div, horizontal scale: 5ms/div

Conclusion

In this paper a new switching table has been proposed for a five level DTC drive to reduce the CMV. The method has been applied in a five-level flying capacitor inverter. The simulation and experimental results show a 60 percent reduction in the amplitude of the CMV without degrading the performance of DTC drive. The generated CMV results in a bearing voltage that will be less than the dielectric breakdown voltage in bearings. Therefore the proposed method is quite effective in reducing the bearing current.

Appendix A

Induction motor specifications

Voltage	400 volt
Power	3kW
Number of pair poles (p)	2
Stator Resistance (Rs)	1.873Ω
Rotor Resistance (Rr)	1.86Ω
Stator and rotor Leakage Inductance Lls=Llr	7.54mH
Main inductance Lm	210mH
Inertial (J)	0.01kg-m2

Direct torque control parameters

Torque hysteresis bandwidth	0.2N.m
Flux hysteresis bandwidth	0.01Wb
Initial and nominal machine flux	0.8Wb
Maximum switching frequency	5000Hz
DTFC sampling	33uS

Appendix B- Power Circuit Design

A low scale multilevel DTC drive for a three-phase induction motor (3kW, 400V), shown in Fig. 11, is designed as follow.

Rectifier Design:

The minimum dc-link voltage to achieve a sinusoidal output with line-to-line RMS voltage of 400V can be calculated as:

$$V_{dc\min} = \sqrt{2}V_{llrms} = 565.7V$$

To determine the nominal dc-link voltage of the converter, a voltage reserve of 6% is assumed good dynamic characteristics (control voltage reserve ≥ 3%)

$$V_{dc} = 1.06 * V_{dc,min} = 600\,V$$

A three-phase full-bridge diode rectifier will be used to provide this dc voltage.

Inverter design:

The maximum ripple should be limited to 7.5V. The maximum ripple is due to the maximum output current:

$$i_C = C\frac{dV}{dt} \rightarrow C = i_C * dt * \frac{1}{dV} = \hat{I}_{ph} * \frac{1}{f_S} * \frac{1}{\Delta V_C}$$

$\hat{I}_{ph}$ = magnitude of the phase current;

ΔV_C = maximum voltage ripple across the flying capacitors.

f_S = switching frequency;

referring to nameplate:

$$I_{ph} = 6.4A \rightarrow \hat{I}_{ph} = \sqrt{2}I_{ph} = 9A$$

Based on (6), the higher carrier frequency results in the smaller flying capacitor. On the other hand, the high speed drives need a high carrier frequency so flying-capacitor topology is competitive with other topologies; for example: $f_S = 5000Hz$. Therefore:

$$C = \hat{I}_{ph} * \frac{1}{f_S} * \frac{1}{\Delta V_C} = 9 * \frac{1}{4800} * \frac{1}{7.5} = 250\mu F$$

Regarding the standard capacitor values, a 220uF is used.

REFERENCES

[1] José Rodríguez, Steffen Bernet, BinWu, Jorge O. Pontt and Samir Kouro, "Multilevel Voltage-Source-Converter Topologies for Industrial Medium-Voltage Drives", IEEE Trans. Indust. Electron., vol. 54, no. 6, Dec. 2007

[2] S. Kouro, M. Malinowski, K. Gopakumar, J. Pou, L. G. Franquelo, B. Wu, J. Rodriguez, M. A. Pérez, and Jose I. Leon, Member, "Recent Advances and Industrial Applications of Multilevel Converters," IEEE Trans. Indust. Electron., vol. 57, no. 8, Aug. 2010

[3] H. Abu-Rub, J. Holtz, J. Rodriguez, and G. Baoming,"Medium-Voltage Multilevel Converters—State of the Art, Challenges, and Requirements in Industrial Applications," IEEE Trans. Indust. Electron., vol.57, no. 8, Aug. 2010

[4] S. S. Fazel, Steffen Bernet, D. Krug, and K. Jalili, "Design and Comparison of 4-kV Neutral-Point-Clamped, Flying-Capacitor, and Series-Connected H-Bridge Multilevel Converters", IEEE Trans. Ind. Applicat., vol. 43, ,pp. 1032-1040, Jul./Aug. 2007.

[5] D. Krug, S. Bernet, S. S. Fazel, K. Jalili, and M. Malinowski, "Comparison of 2.3-kV Medium-Voltage Multilevel Converters for Industrial Medium-Voltage Drives", IEEE Trans. Indust. Electron., vol.. 54, no. 6, Dec. 2007

[6] K.B. Lee, J.H. Song, I. Choy, and J.Y. Yoo, "Torque Ripple Reduction in DTC of Induction Motor Driven by Three-Level Inverter With Low Switching Frequency", IEEE Trans. Power Electron., vol. 17, no.2, Mar. 2002.
[7] J. Rodríguez, J.Pontt, S. Kouro, and P. Correa, "Direct Torque Control with Imposed Switching Frequency in an 11-Level Cascaded Inverter", IEEE Trans. Indust. Electron., vol. 51, Aug. 2004 pp. 827-833.
[8] M.F. Escalante, J.-C. Vannier and A. Arzande, "Flying capacitor multilevel inverters and DTC motor drive applications", IEEE Trans. Indust. Electron., vol.49, Aug. 2002, pp.809 – 815.
[9] J. Erdman, R. Kerkman, and D. Schlegel, "Effect of PWM inverters on AC motor bearing currents and shaft voltages," IEEE Trans. Ind. Applicat., vol. 32, no. 2, pp. 250–259, Mar./Apr. 1996.
[10] S. Chen, T. A. Lipo, and D. Fitzgerald, "Modelling of bearing currents in inverter drives," IEEE Trans. Ind. Applicat., vol. 32, no. 1, pp. 21–32, Jan./Feb. 1996.
[11] Busse, D., Erdman, J. M., Kerkman, R. J., Schlegel, D. W. and Skibinski, G. L. (1997c), "An evaluation of the electrostatic shielded induction motor: a solution for rotor shaft voltage buildup and bearing current," IEEE Trans. Ind. Applicat., vol. 33, no. 6, Nov./Dec.97
[12] Fei Wang, "Motor shaft voltages and bearing currents and their reduction in multilevel medium-voltage PWM voltage-source-inverter drive applications", IEEE Trans. Ind. Applicat., vol. 36, Issue:5, Sep./Oct. 2000, pp. 1336 – 1341.
[13] Xiyou Chen, Dianguo Xu, Fengchun Liu, Jianqiu Zhang, "A Novel Inverter-Output Passive Filter for Reducing Both Differential- and Common-Mode dv/dt at the Motor Terminals in PWM Drive Systems," IEEE Trans. Indust. Electron., vol. 54, no. 1, pp. 419-426, Feb. 2007.
[14] Hanigovszki, Norbert ; Poulsen, Joern ; Blaabjerg, Frede . "A Novel Output Filter Topology to Reduce Motor Overvoltage," IEEE Trans. Ind. Applicat., vol. 40, no. 3 pp. 845-852, May/Jun. 2004.
[15] Hirofumi Akagi and Shunsuke Tamura, "A Passive EMI Filter for Eliminating Both Bearing Current and Ground Leakage Current From an Inverter-Driven Motor," IEEE Trans. Power Electron., vol. 21, no. 5, Sep. 2006
[16] D. Hyypio, "Mitigation of Bearing Electro-Erosion of Inverter-Fed Motors Through Passive Common-Mode Voltage Suppression," IEEE Trans. Ind. Applicat., vol. 41, no. 2, pp. 576–583, Mar./Apr. 2005.
[17] C. Mei, J. C. Balda, W. P. Waite, "Cancellation of Common-Mode Voltages for Induction Motor Drives Using Active Method," IEEE Trans. Energy Convers., vol. 21, no. 2, Jun. 2006
[18] H. Zhang et al, "Multi-level inverter modulation schemes to eliminate common-mode voltages," IEEE Trans. Ind. Applicat., vol. 36, pp. 1645-1653, Nov./Dec. 2000.
[19] P.C. Loh, D.G. Holmes, Y. Fukuta & T.A. Lipo, "A Reduced Common Mode Hysteresis Current Regulation Strategy for Multilevel Inverters," IEEE Trans. Power Electron.,vol. 19, pp. 192-200, Jan. 2004
[20] R. S. Kanchan, P. N. Tekwani, and K. Gopakumar, "Three level inverter scheme with common mode voltage elimination and dc link capacitor voltage balancing for an open-end winding induction motor drive," IEEE Trans. Power Electron., vol.21, no.6, pp. 1676-1683", Nov. 2006
[21] W. Leonhard, "Control of Electrical Drives," Third edition, Berlin, Springer, 2001.
[22] Arasteh M., Rahmati, A., Farhangi, S., Abrishamifar, A., "DTC on multilevel inverters for pumping and ventilation applications," 4th IEEE Conference on Industrial Electronics and Applications, ICIEA 2009. 25-27 pp. 2316 – 2320, May 2009.
[23] A. Muetze and A. Binder, "Calculation of motor capacitances for prediction of the voltage across the bearings in machines of inverter-based drive systems," IEEE Trans. Ind. Applicat., vol. 43, no. 3, pp. 665–672,May/Jun. 2007.

Authors:
Mohammad Arasteh: Phd.Student, marasteh@iust.ac.ir, School of Eectrical Engineering, Iran University of science and technology, Narmak, Tehran, Iran.
Abdolreza Rahmati, Associate Professor, rahmati@iust.ac.ir, School of Eectrical Engineering, Iran University of science and technology, Narmak, Tehran, Iran.
Shahrokh Farhangi, Associate Professor,farhangi @ ut.ac.ir, School of Electrical & Computer Engineering, Tehran university,north amirabad, Tehran, Iran
Adib abrishamifar: Assistant Professor, abrishamifar@iust.ac.ir, School of Eectrical Engineering, Iran University of science and technology, Narmak, Tehran, Iran.